Research Article | Vol. 16, No. 7 / 1 Jul 2026 / Optical Materials Express 2080
Optical Materials EXPRESS

Transparency versus Anderson localization in one-dimensional disordered stealthy hyperuniform layered media

MICHAEL A. KLATT,[1,2,3] PAUL J. STEINHARDT,[4,*] AND SALVATORE TORQUATO[4,5,6,7]

[1]German Aerospace Center (DLR), Institute for AI Safety and Security, Wilhelm-Runge-Str. 10, 89081 Ulm, Germany
[2]German Aerospace Center (DLR), Institute of Frontier Materials on Earth and in Space, Functional, Granular, and Composite Materials, 51170 Cologne, Germany
[3]Department of Physics, Ludwig-Maximilians-Universität München, Schellingstr. 4, 80799 Munich, Germany
[4]Department of Physics, Princeton University, Princeton, New Jersey 08544, USA
[5]Department of Chemistry, Princeton University, Princeton, New Jersey 08544, USA
[6]Princeton Materials Institute, Princeton University, Princeton, New Jersey 08544, USA
[7]Program in Applied and Computational Mathematics, Princeton University, Princeton, New Jersey 08544, USA
[*]steinh@princeton.edu

Abstract: Wave transport in one-dimensional (1D) systems, even with an arbitrarily small amount of disorder, is conventionally expected to exhibit localization at all frequencies. A recent strong-contrast expansion for the effective dynamic dielectric constant of disordered stealthy hyperuniform 1D (layered) two-phase dielectric media, exact through third order, predicts optical transparency over a continuous frequency band up to ω_c, in agreement with simulations of systems containing a small number (50) of thin slabs. In this paper, we analyze simulations with up to 10,000 slabs and find no apparent evidence that higher-order terms induce Anderson localization or deviations from transparency over a continuous band extending from zero to a frequency $\omega_T \lesssim \omega_c$, consistent with a tight upper bound predicted by the strong-contrast formula. We employ a transfer-matrix method to compute Lyapunov exponents, which we demonstrate is a more sensitive probe of Anderson localization by applying it to systems known to exhibit localization. The Lyapunov exponents show clear evidence of localization for layered media with ordinary disorder, but no such evidence when slabs are arranged periodically or in a disordered stealthy hyperuniform pattern. Although it remains challenging to determine whether 1D disordered stealthy hyperuniform layered media possess a finite localization length on scales beyond our already large system sizes, these findings may have practical implications for photonic and phononic material design.

Published by Optica Publishing Group under the terms of the Creative Commons Attribution 4.0 License. Further distribution of this work must maintain attribution to the author(s) and the published article's title, journal citation, and DOI.

1. Introduction

Anderson localization is a fundamental phenomenon in which wave transport of all kinds (fermionic, phononic, or electromagnetic) is halted due to multiple scattering that traps waves within a bounded region [1,2]. According to the standard lore, this localization effect occurs in three-dimensional (3D) systems only if the degree of disorder is above a critical threshold; however, for one-dimensional (1D) systems, even an arbitrarily small amount of disorder leads to localization for all frequencies [3]. Random dimers are a well-known exception [4] but, importantly, they are transparent to light propagation only for a discrete set of resonant frequencies

#578221 https://doi.org/10.1364/OME.578221
Journal © 2026 Received 4 Sep 2025; revised 29 May 2026; accepted 1 Jun 2026; published 17 Jun 2026

Optical Materials EXPRESS

due to constructive interference between identical sites comprising each dimer pair, not for a continuous band of frequencies. To date, examples of continuous frequency bands of perfect transparency have not been rigorously demonstrated for any disordered 1D layered medium.

Motivated by recent theoretical studies [5,6], we present here comprehensive numerical studies of localization and transparency for the case of electromagnetic waves propagating in 1D layered systems consisting of a disordered stealthy hyperuniform sequence of thin parallel slabs with a high dielectric constant separated by intervals with low dielectric constant. We compute the propagation of electromagnetic waves at normal incidence through up to 10,000 slabs [7,8] and find no apparent evidence of Anderson localization for a continuous band of frequencies between zero and some critical value ω_T, similar to what we obtain for perfectly periodically spaced slabs over the same frequency range. In stark contrast, our equivalent studies of conventionally disordered layered systems that are neither stealthy nor hyperuniform exhibit clear evidence of localization and deviation from transparency even when their degree of disorder is much lower than the disorder in our stealthy hyperuniform examples. Figure 1 is a schematic representing our transparency versus localization results for different types of ordered and disordered layered media.

Disordered stealthy hyperuniform many-particle systems are a special subclass of hyperuniform amorphous states of matter [9] with an array of physical properties that cannot be achieved by nonstealthy hyperuniform or by nonhyperuniform disordered media [10]. They are defined by a structure factor $S(\mathbf{k})$ that is exactly zero for a continuous band of wavenumbers $k \equiv |\mathbf{k}|$ around the origin ($0<k<K$) [11], like a crystal, and yet exhibit diffuse (isotropic) scattering for $k>K$, unlike a crystal [10]. The fact that no single scattering can occur from infinite to intermediate wavelengths ($O(2\pi/K)$) imposes a continuum of constraints on the disorder, forcing it to be highly correlated across the sample and to satisfy the bounded-hole property [12,13], which it shares with periodic structures. It has been suggested [10] that the hybrid crystal-liquid nature of disordered stealthy hyperuniform materials endows them with unique and often optimal properties, including remarkable photonic [5,6,14–25] and phononic [26–30] characteristics, especially the formation of band gaps [14,21,22], transport properties [31,32] and mechanical properties [32]. In particular, transparency and Anderson localization has been intensively studied in two- and three-dimensional stealthy hyperuniform systems [15,16,19,23,33].

While most of the aforementioned studies examined the unusual properties of 2D and 3D disordered stealthy hyperuniform materials, recent theoretical work [5,6] has revealed unexpected localization properties in such 1D media. Specifically, a quantitative theoretical formula has been derived in Ref. [5] for the effective dynamic dielectric constant based on a nonlocal strong-contrast formalism developed in Ref. [34] for general microstructures across space dimensions and various structural symmetries. Importantly, the fact that the structure factor $S(k)$ equals zero for a range $0<k<K$ does not guarantee transparency in 1D systems. The stealthy condition implies the absence of single-scattering events, but it does not rule out multiple-scattering processes that can lead to a finite scattering mean free path [15,23]. Because of the fast-convergence properties of strong-contrast expansions, lower-order truncations yield closed-form approximate formulas for the effective dielectric constant that apply well beyond the quasistatic regime, *i.e.*, they accurately estimate the higher-order contributions in the remainder term for a broad range of incident wavenumbers. In particular, the resulting formula truncated at third order predicts that 1D disordered stealthy hyperuniform layered media have perfect transparency (no Anderson localization) for a range of frequencies and specifies a tight upper bound $\omega_c \gtrsim \omega_T$ [5,6]. The predictions of the strong-contrast formula were also shown to agree with finite-difference time-domain (FDTD) simulations for 5000 renditions of small systems consisting of up to 50 high-dielectric slabs [6]. It was conjectured that any finite localization length would be large compared to any practically large sample size in the transparency interval. However, simulations of 50 slabs are far too small to provide convincing evidence.

Optical Materials EXPRESS

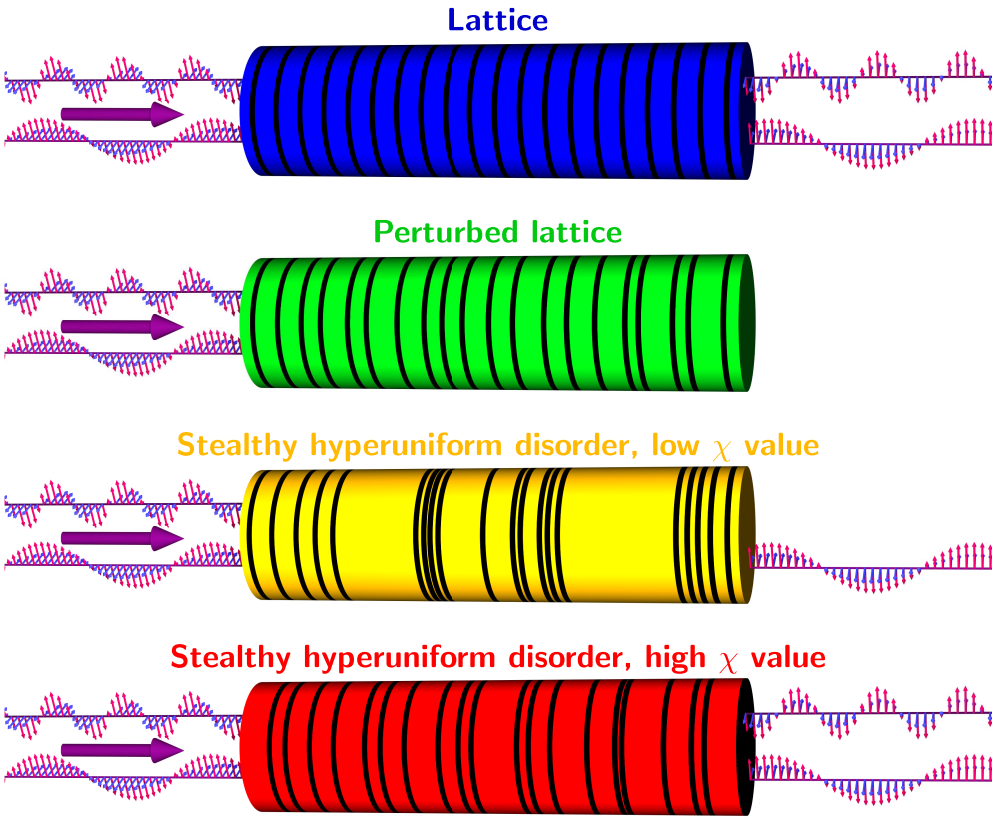


Fig. 1. Schematic of transparency vs Anderson localization in layered media that consist of thin high-dielectric slabs (represented by black layers) and a low-dielectric material in between (represented by colored layers). Different colors are used for different models: Whereas a lattice is transparent to waves at most frequencies (top panel), even a slight perturbation leads to localization and hence no transport (second panel). A similar schematic for equiluminous or RSA would show the same outcome. In contrast, disordered stealthy hyperuniform media have a high degree of local disorder, but they are transparent even for large system sizes for frequencies $\omega<\omega_T$, where ω_T is directly proportional to the magnitude of χ, a dimensionless measure of the range of the wavenumbers in which single scattering in the two-phase medium is completely forbidden. Hence, the disordered stealthy hyperuniform pattern with high χ (fourth panel) will be transparent to high frequencies which are localized for low χ (third panel). The schematic is consistent with the numerical results shown in Fig. 2.

Here, we analyze 100 renditions of samples consisting of up to 10,000 high-dielectric slabs using advanced, state-of-the-art simulation techniques, including the utilization of Lyaponov exponents and a novel minimization procedure to eliminate ripple effects. This allows the transparency properties to be compared quantitatively with samples known to have no localization (perfectly periodic lattices) and those known to exhibit Anderson localization (perturbed periodic lattices). We observe an apparent transparency regime for disordered hyperuniform systems that is clearly distinct of the perturbed periodic lattice, comparable to that of the perfectly periodic lattice, and in remarkable accord with the tight upper bound given in [5], even for the largest system sizes and for strong dielectric contrasts. These findings further indicate that the effects of

Optical Materials EXPRESS

wave propagation in disordered stealthy hyperuniform systems are qualitatively different from other known cases of disorder.

In this transparency regime, our disordered stealthy hyperuniform samples behave very similar to perfectly periodically spaced slabs for all frequencies less than ω_T. On the other hand, unlike the case of periodically spaced slabs, our disordered stealthy hyperuniform samples exhibit a sharp transition to a localized regime for $\omega>\omega_T$, where ω_T is close to but always strictly below ω_c, the upper bound prediction based on the strong-contrast formalism [5]. Furthermore, the dependence of ω_T on the dielectric contrast, volume fraction and degree of stealthiness (*i.e.*, the value of χ as defined below) is also in very good agreement with the theoretical predictions for ω_c in [5]; see Figs. 2 and 3. In stark contrast, the *perturbed* (periodic) lattices exhibit no transparency regime and a localization length less than the sample size, despite the fact that the perturbed periodic samples are *less disordered* than the stealthy hyperuniform ones (as quantified by the τ-order metric).

We pay close attention to limitations due to system size, numerical accuracy and boundary conditions (especially oscillations known as ripple effects, which play an important role in the analysis, as described below). We mitigate these effects using various techniques, *e.g.*, via a QR decomposition (see Methods), averages with high statistics, and moving windows. We extend these methods to continuous functions of the system size L, which allows us to observe sharp peaks for both the crystal and disordered stealthy hyperuniform samples. We conclude that the localization length is much larger than the large sample sizes that we have studied. Indeed, as is dramatically illustrated in Figs. 4 and 5, our results for disordered stealthy hyperuniform layered media are remarkably similar to the regime of perfect transparency obtained for layered media with perfectly periodic spacing which obviously have infinite localization length. Hence, our findings support the notion that one-dimensional disordered stealthy hyperuniform systems are qualitatively different from other layered systems with ordinary types of disorder. That said, we must caution that the strong-contrast formula is accurate but approximate and the computational results are limited by numerical noise. Hence, one must be cautious in extrapolating our results to much larger size, dielectric contrast, or volume fraction, as elaborated in the Discussion section.

We note that there has been related recent work on localization effects in disordered stealthy hyperuniform layered media by Park et al. [35], but they did not focus on the transparency properties. Also, Meek and Florescu [24,25] discussed localization in the context of photonic band gaps in disordered stealthy hyperuniform layered media using the inverse participation ratio to analyze the spatial extent and spectral composition of the modes in layered media. Vibrational behaviors of 1D stealthy hyperuniform samples have been studied previously [27,29], but without focusing on Anderson localization vs transparency. As indicated above, tranparent and localized phases have also been found in two- and three-dimensional stealthy hyperuniform systems [15,16,19,23,33]; see also the description in the Discussion section.

2. Models

Our models are 1D layered media consisting of two-phases: high-dielectric thin slabs that are embedded within a low-dielectric material. The models span a broad range of local and global disorder and order, from ordinary disordered (non-stealthy and non-hyperuniform) to a perfectly ordered lattice. For each model, we start from a 1D point process on the line with number density ρ [36]. We then center at each point high-dielectric slabs with equal thickness b and fill the spaces between with a low-dielectric material. The volume fraction occupied by the high-dielectric material is $\phi = \rho b$. We choose the unit of length such that $\rho = 1$, which means that the thickness b of each slab equals ϕ. Importantly, we only consider point processes with a distance $\geq \phi$ between points to avoid overlapping slabs. Such overlap would, *e.g.*, result in a non-stealthy layered medium even if the point process was stealthy hyperuniform [10]. The spaces between slabs may vary depending on the underlying point process. We consider the following cases:

Optical Materials EXPRESS

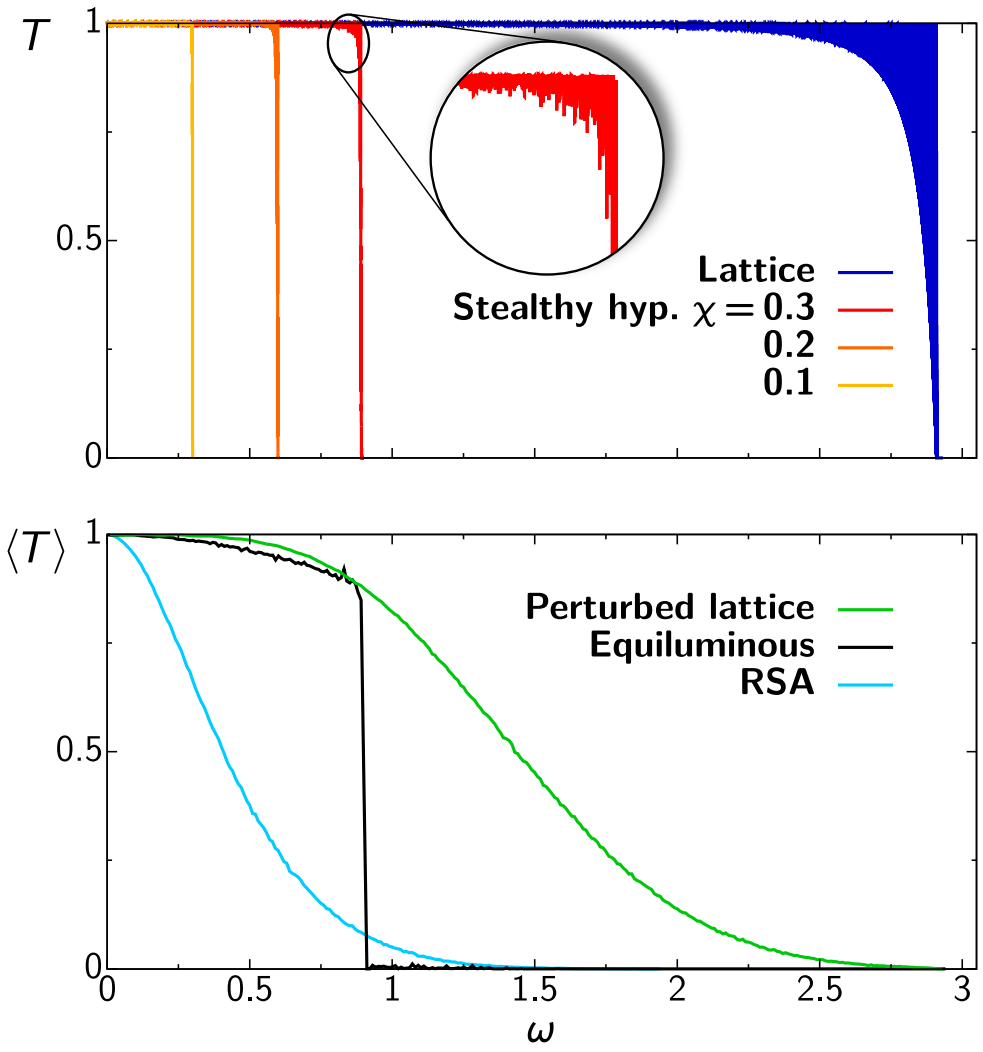


Fig. 2. Top panel: transmission T through single samples of a lattice with periodically spaced slabs (rightmost) compared to disordered stealthy hyperuniform layered media with different values of χ indicating that they exhibit qualitatively similar behavior: a sharp transition between a transparent and localized regime. (Here, we only show data up to ω_T for each case to avoid confusion with noise in the localized regime at larger ω, as discussed in [47].) The transmission for the lattice has very high frequency oscillations in T (the ripple effect) that appear like a kind of shading at $\omega \to \omega_T$ at this resolution; the inset shows that the disordered stealthy hyperuniform medium exhibits a similar behavior. Bottom panel: transmission for layered media with other types of disorder (perturbed lattice, equiluminous, and RSA) each exhibiting localization such that $T<1$ for all $\omega>0$. The curves are an average over 100 samples. Each sample in the top and bottom panels consists of $N = 10,000$ slabs with $\varepsilon_2 = 9$ and $\varepsilon = 1$. We use the same dielectric constants for the incident and substrate medium, respectively.

Optical Materials EXPRESS

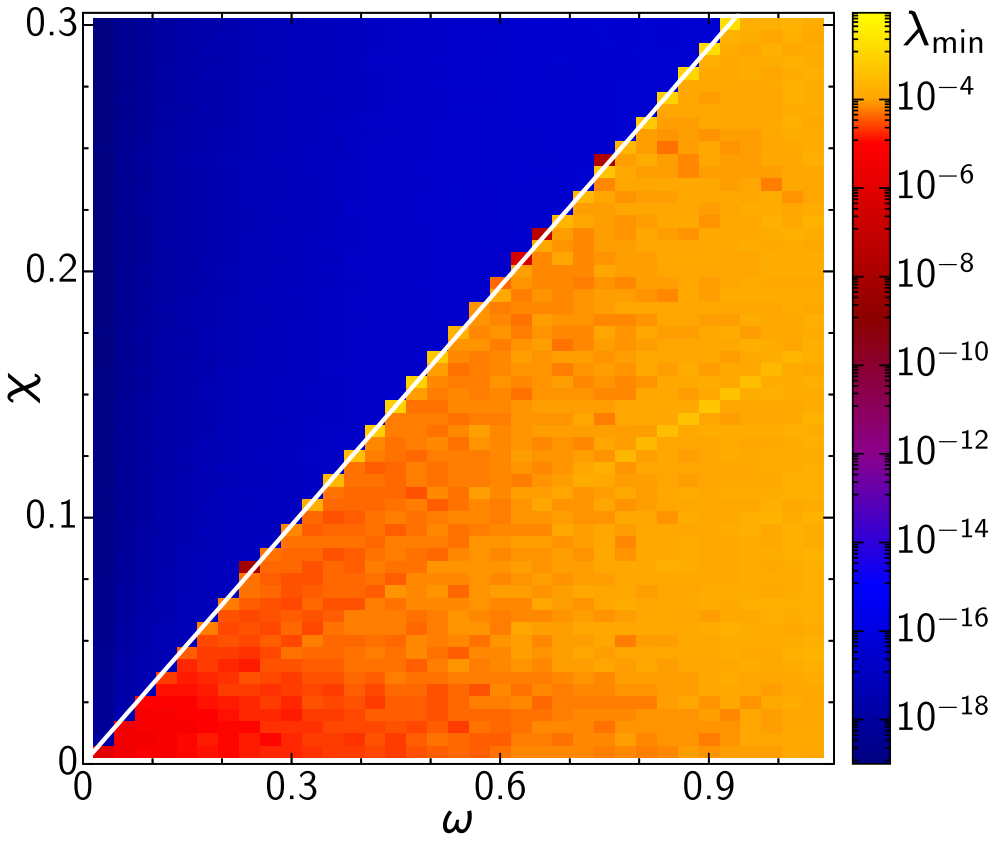


Fig. 3. The 'phase diagram' of the Lyapunov exponent $\lambda_{\min} = 1/\xi$ for the disordered stealthy hyperuniform samples reveals a sharp transition in agreement with the theoretical prediction in [5] (solid line).

(1) The *lattice* composed of equally spaced slabs represents perfect order due to perfect periodicity.

(2) In a *perturbed lattice* with perturbation strength a, the position of each point (and hence high-dielectric slab) is independently and randomly varied by an amount that is uniformly distributed within the interval $(-a, a)$. To avoid overlaps, $a<1-\phi$. In our case, $a = 0.1$ and $\phi = 1\%$. A perturbed lattice is hyperuniform but not stealthy [9].

(3) *Random sequential adsorption (RSA)* is non-hyperuniform, and it guarantees non-overlapping slabs [10,36,37].

(4) We create *disordered stealthy hyperuniform* layered media using the collective-coordinate optimization procedure to obtain disordered ground states with $\chi<1/3$ from random initial conditions [11]. To avoid overlapping slabs, we modify the standard stealthy potential to include a soft-core repulsion as in [38,39]. The degree of stealthiness for underlying point process is measured by the χ value, which is proportional to the ratio of the reciprocal space volume of wave vectors with constrained values to the total number of degrees of freedom. In one dimension, $\chi := K/(2\pi\rho)$, where K is the upper limit on the constrained wavenumbers, *i.e.*, $S(k) = 0$ for $0<k<K$ [40]. In practice, due to the limits of numerical precision, we generate high-quality stealthy samples with values of $S(k)<10^{-20}$ for $0<k<K$, which corresponds to a spectral density $\tilde{\chi}_v(k)$ for the resulting stealthy two-phase medium [37] that is less than 10^{-24}. The spectral density $\tilde{\chi}_v(k)$ for a distribution of identical nonoverlapping slabs in a matrix is directly determined

Optical Materials EXPRESS

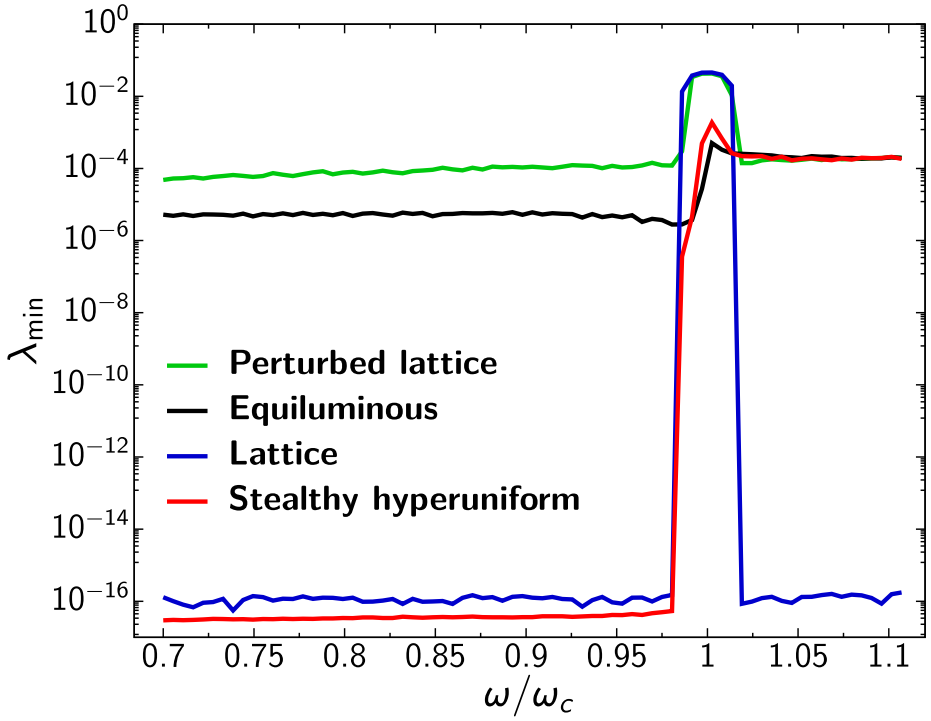


Fig. 4. Minimal Lyapunov exponent $\lambda_{\min}$ as a function of frequency ω rescaled by ω_c of the strong-contrast formula (3): as expected, we observe a transparency regime for the lattice but localization at all frequencies for the perturbed lattice. Surprisingly, the disordered stealthy hyperuniform samples exhibit an apparent transparency regime, like for the integer lattice, up to $\omega = \omega_T \approx \omega_c$, where we observe a sharp transparency-to-localization transition.

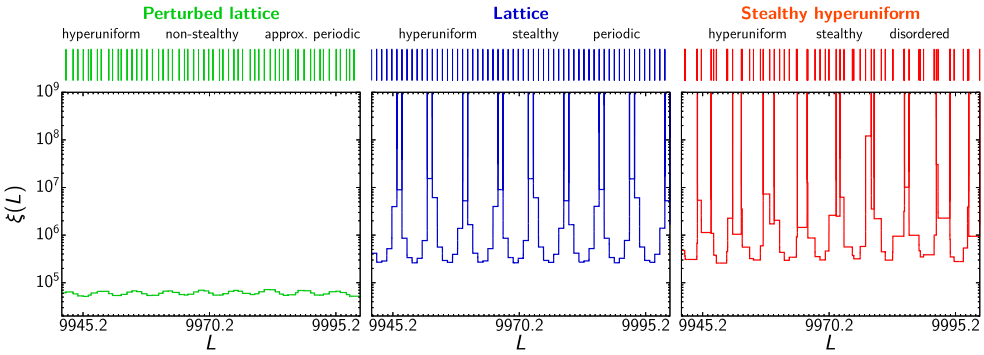


Fig. 5. Localization length $\xi(L)$ as a function of the system size L that varies over about the last 60 slabs for single samples using $\varepsilon_2 = 9$, $\phi = 1\%$, and $\omega = 0.5\omega_c$ for $\chi = 0.3$; corresponding portions of the samples are shown above the plots of $\xi(L)$. For the perturbed lattice (left), we observe a finite localization length for all continuously varied values of L. In contrast, for the integer lattice (center), the localization length strongly varies due to the ripple effect, and within some of the high-dielectric slabs, the localization length diverges in sharp peaks. The disordered stealthy hyperuniform sample (right) behaves analogously to the lattice. Despite the ripple effect, which causes oscillations, $\xi(L)$ remains larger than the system size (with about the same lower values for the lattice and the disordered stealthy hyperuniform sample). The approximate periodicity in $\xi(L)$ corresponds to ω. Recall that $1/\rho$ defines the unit of length.

Optical Materials EXPRESS

by $S(k)$ associated with center points of the slabs [41]; see also the Supplement 1 text for the relevant formulas.

(5) For comparison, we also construct layered media from *equiluminous* point distributions [11] with a constant positive value of the structure factor $S(k) = 10^{-2}$ for $0<k<K$, which corresponds to a spectral density $\tilde{\chi}_V(k)$ of about 10^{-6} in the same wavenumber range.

For each model, we simulate samples with 10,000 slabs. For obtaining the number of samples (mostly 100 per model), see the Methods section.

Table 1 lists, as a natural metric of local order, the standard deviations σ of the intervals separating the high-dielectric slabs. Disordered stealthy hyperuniform layers with $\chi = 0.1$ have about the same value of σ as the ideal gas. Even for $\chi = 0.3$, we observe the same order of magnitude with $\sigma = 0.637$. For the perturbed lattice, we choose a perturbation strength of $a = 0.1$ such that σ is about an order of magnitude smaller than for our disordered high-χ stealthy hyperuniform samples. That is, our perturbed lattice model has a higher degree of order across all length scales as measured by the τ-order metric [40] (see also Table 1 and the Supplement 1) or when compared to disordered stealthy hyperuniform layered media in the classical sense of variations in the intervals filled with low-dielectric material.

Table 1. Standard deviation σ of the intervals between high-dielectric slabs as a natural metric for local disorder in our models, and the τ-order metric for order across all scales evaluated at the maximal system size of $L = 10,000$

Model	Stealthy hyperuniformity			Equiluminous	RSA	Perturbed lattice	Lattice
	$\chi = 0.1$	$\chi = 0.2$	$\chi = 0.3$			$a = 0.1$	
σ	1.08	0.793	0.637	0.600	0.600	0.0816...	0
$\tau(L)$	3.5	3.7	4.5	0.89	1.15	23,332	∞

3. Transfer matrix method and Lyapunov exponents

We compute the wave transport through the dielectric layered media for all of the models above using the classic transfer matrix method [7,8], which is exact under standard assumptions such as homogeneous dielectric materials [42,43]. In our calculations, we assume loss-free transport, normal incidence, and a dielectric contrast of $\varepsilon_2/\varepsilon_1$ between the high- and low-dielectric materials. For the low-dielectric material, we use $\varepsilon_1 = 1$ as for air or the vacuum. For the volume fraction of the high-dielectric slabs, we choose $\phi = 1\%$, which allows for strong local disorder in the stealthy hyperuniform samples. The unit of time is defined by setting the vacuum speed of light to one.

We begin by evaluating the transmission coefficient T; for details on the setup, see the Methods section. For a sensitive localization analysis, we then compute the finite approximation of the Lyapunov exponents for a sample of length L [44,45]:

$$\lambda(L) := \left\langle \frac{1}{L} \log \|\Pi(L)\| \right\rangle, \tag{1}$$

where $\|\Pi(L)\|$ is the spectral norm (*i.e.*, largest singular value) of the product of transfer matrices $\Pi(L)$, and the angular brackets indicate an ensemble average. Note that the localization analysis is independent of the chosen norm (since for a finite-dimensional complex vector space, every pair of norms is equivalent); hence our analysis of the Lyaponov exponent is (up to rescaling) equivalent to studying the average of $\ln T$ [45]. To avoid numerical instabilities in the multiplication of 20,000 matrices, we here choose the spectral norm and use a QR-decomposition [44,46]; see the Method section for details.

Optical Materials EXPRESS

The Lyapunov exponent is then defined in the limit:

$$\lambda := \limsup_{L\to\infty} \lambda(L), \tag{2}$$

and the localization length as its inverse, $\xi := 1/\lambda$. For the non-stealthy disordered systems (perturbed lattice, equiluminous, and RSA), we observe within our numerical and statistical accuracy a convergence of $\lambda(L)$ to a positive value $\lambda>0$ (in agreement with the expected self-averaging property of the largest Lyaponov exponent). For the perturbed lattice, the value of λ can be deduced via an extrapolation. In contrast, the limit $\lambda = 0$ and hence $\xi = \infty$ cannot be rigorously evaluated from our finite system sizes. We can only compare the finite approximations $\lambda(L)$ and $\xi(L) := 1/\lambda(L)$ for the stealthy hyperuniform system to those of the lattice, for which we know that $\lambda = 0$ and hence $\xi = \infty$.

Note that instead of computing the Lyapunov exponents for discrete steps (namely single layers), we use the length of the sample as a normalization and can thus compute the exponents for any finite interval of our samples, *i.e.*, we can smoothly vary the system size L and study λ as a continuous function of L.

4. Results

To gain an intuitive understanding of the main phenomenon, we begin with a study of the transmission coefficient T before discussing the more careful localization analysis based on the Lyaponov exponent, which is equivalent to studying the average of $\ln T$ [45]. We first consider the transmission through a periodic layered medium, based on the integer lattice; see Fig. 2 (top panel, blue curve). When numerically resolved, the transmission coefficient T can be seen to exhibit rapid oscillations caused by the boundary conditions, an interference phenomenon known as ripple effect [8]. However, T (when numerically resolved) returns to unity for all frequencies up to a sharp transition at a critical frequency ω_T, which defines the edge of the first photonic band gap (PBG) [42,48,49]. Within the photonic band gap, we observe strong (numerical) noise as is characteristic for localization [47]. For our three disordered stealthy hyperuniform samples with different values of χ, we observe the same qualitative behavior consistent with the strong-contrast expansion in [5]: apparent transparency up to a critical frequency ω_T, as shown in the top panel of Fig. 2, that includes a ripple effect (see inset). Importantly, we observe no dependence of the transparency regime on the number of slabs as it ranges from 1000 to 10,000.

This transparency behavior of the perfect lattice and the disordered stealthy hyperuniform samples in the top panel of Fig. 2 contrasts sharply with that for layered media based on disordered but non-stealthy configurations (perturbed lattice, equiluminous or RSA), as shown in the bottom panel of Fig. 2. Comparing a perturbed lattice to RSA, there is only a quantitative difference in the decay rate (which increases with system size), but we find the same qualitative behavior, specifically, no sharp transition. For the equiluminous samples, the behavior is similar to the perturbed lattice up to ω_T for the stealthy hyperuniform. In no case is there a range of ω for which these non-stealthy disordered media are transparent.

It is especially notable that one can clearly detect localization for the perturbed lattice in the bottom panel of Fig. 2 but not for the disordered stealthy hyperuniform samples shown in the top panel even though, as mentioned above, the perturbed lattice has more local order as measured by the τ-order metric [40] or σ of the intervals separating the high-dielectric slabs; see Table 1.

Returning to the top panel of Fig. 2, the only obvious difference in the behavior of T for the perfectly periodic lattice and the disordered stealthy hyperuniform samples is the value of the threshold $\omega_T(\chi, \varepsilon_2, \varepsilon_1, \phi)$, which varies with the values of χ, the dielectric contrast and the volume fraction. Consistent with previous theoretical results [5] and small scale simulations from Ref. [5,38], we find that the strong-contrast approximate formula provides a reliable upper

Optical Materials EXPRESS

bound on the transparency-to-localization threshold ω_T:

$$\omega_T \lesssim \omega_c(\chi; \varepsilon_2, \varepsilon_1, \phi) = \frac{\pi\chi}{\sqrt{\phi(\varepsilon_2 - 1) + \varepsilon_1}}. \tag{3}$$

This bound is rather tight – that is, $\omega_T/\omega_c \approx 1$ in all our samples – and becomes sharp in the weak-contrast limit where $\omega_T/\omega_c \to 1^-$. (The weak-field behavior is due to the fact that the nonlocal strong-contrast expansion converges rapidly and is highly accurate whenever there is coherent wave transport.)

Since we know that the lattice has a transparency regime with an infinite localization length and hence a vanishing Lyapunov exponent, we have to compensate for the ripple-like oscillations in the transmission plot. For this purpose, we minimize $\lambda(L)$ over a small range of $L \in [9900, 10000]$ that preserves the order of magnitude of the sample. Since the oscillations may vary with shifts of the samples (due to the non-periodic setup of the transfer matrix calculations), we use the median over about 40 shifts per sample for a representative value of $\lambda_{\min}$, which proves to provide a good approximation for λ for the lattice in the thermodynamic limit; for further discussions and details on the minimization algorithm, see the Methods section.

In Fig. 3, we have systematically studied the frequency- and χ-dependence of the transparency-to-localization transition for disordered stealthy hyperuniform layered media with χ<0.3 to produce a corresponding 'phase diagram' of $\lambda_{\min}(\omega, \chi)$ for $\varepsilon_2 = 4$. The figure shows a sharp boundary between a transparent regime with λ_N<10^{-15} (like for a lattice) and a localized regime with $\lambda_N \approx 10^{-3}$ (like for RSA). The critical frequency ω_c as a function of the χ value is in good agreement with the strong-contrast formula from (3) (indicated by the solid line).

Figure 4 provides another way to visualize the transparency regime for the lattice (with $\chi = 1$), where $\lambda_{\min}$ vanishes up to floating point precision for ω<$\omega_T \approx 0.98\omega_c$. Remarkably, for the same form of visualization, the disordered stealthy hyperuniform samples with $\chi = 0.3$ exhibit an apparent transparency regime that cannot be distinguished numerically from that of the lattice: $\lambda_{\min}$ vanishes up to floating point precision. This stands in stark contradistinction to the standard Anderson localization lore but in accord with the predictions of the strong-contrast formula.

As a comparison, we find an exponentially larger value of $\lambda_{\min}$ (or small localization length $\xi = 1/\lambda_{\min}$) at all frequencies for the perturbed lattice in agreement with the standard lore of Anderson localization. The same localization behavior is found for the equiluminous samples in which $S(k) = 10^{-2}$ for 0<k<K. This result for the equiluminous case demonstrates that a modest suppression of $S(k)$ over the range 0<k<K is not sufficient to attain transparency.

Beyond the transparency regime, i.e., for ω>ω_T, the lattice behaves differently from the stealthy hyperuniform disordered medium as is evident in Fig. 4. The lattice exhibits a PBG (approximately symmetric around ω_c) followed by a second transparency regime; for the disordered stealthy hyperuniform samples, we observe localization for any ω>ω_T that we considered. Put differently, in contrast to the lattice, the disordered stealthy hyperuniform samples appear to be fundamentally different in that their transparency regimes behave as low-pass filters.

To understand the transparency regime in more detail, we next consider $\xi(L) = 1/\lambda(L)$ for individual configurations. Figure 5 shows $\xi(L)$ for about 60 slabs close to $L = 10,000$ with $\varepsilon_2 = 9$ and $\phi = 1\%$. We compare the results for a periodic lattice, a perturbed lattice, and a disordered stealthy hyperuniform layered medium, assuming the same input frequency $\omega \approx 0.453$, which corresponds to $\omega = 0.5\omega_c$ for $\chi = 0.3$. At the center panel are the results for the perfect integer lattice, where we know that we are in the transparency regime. We observe a complex, approximately periodic function. Consistent with the ripple effect, the approximate periodicity of the strong oscillations is set by the frequency ω. The localization length $\xi(L)$ only changes inside the high-dielectric phase and remains approximately constant in the low-dielectric phase, which leads to a 'staircase appearance' with rises in the slabs and runs between. In certain high-dielectric slabs, $\xi(L)$ diverges in sharp peaks, consistent with the perfect transparency of the lattice at this frequency.

Optical Materials EXPRESS

On the left hand panel of Fig. 5, the behavior for the perturbed lattice is qualitatively different. We find weak oscillations with the same periodicity as for the lattice, but there are no points of diverging ξ or even finite $\xi \gg L$. We only find $\xi<L$, i.e, the localization length is less than the system size for all shifts. The right panel shows the results for the disordered stealthy hyperuniform sample, where we observe qualitatively the same behavior as for the lattice. The high-dielectric slabs are strongly disordered leading to stronger fluctuations in $\xi(L)$ but still with the same approximate periodicity. For the lattice, we always observe pairs of sharp peaks in neighboring high-dielectric slabs. For the disordered stealthy hyperuniform layered media, we also observe pairs of sharp peaks, but not necessarily in neighboring slabs.

5. Discussion

As noted in the introduction, disordered stealthy hyperuniform layered media have unusual long-range correlations compared to typical disordered systems, and, as a consequence, are not subject to Anderson localization theorems that assume uncorrelated disorder [45,50,51]; nor do they conform to the conditions assumed in theorems that consider certain kinds of correlated disorder, such as [52]. However, the mere fact that the structure factor $S(k)$ equals zero for a range of wavenumbers does not guarantee transparency in 1D systems. It only implies the absence of single-scattering events, but multiple-scattering processes can lead to strong localization. Here, we find through highly precise numerical analyses that the one-dimensional disordered stealthy hyperuniform samples are the only disordered layered media among those tested that exhibit an apparent transparency behavior over 10,000 slabs that, as illustrated in Fig. 4, is similar that of a perfect lattice that is known to be perfectly transparent in the thermodynamic limit. More precisely, for the accessible large system size of 10,000 high-dielectric slabs, the disordered stealthy hyperuniform samples exhibit, within our numerical accuracy, a continuous transparency regime for $\omega<\omega_T \lesssim \omega_c$ that is in excellent agreement with the strong-contrast formula in [5]. The clear signature of localization observed for the perturbed lattice and the equiluminous samples in Fig. 4 suggests that relatively small deviations of any kind from stealthiness destroy perfect transparency.

This observation explains why there are limitations on how far one can go in exploring transparency in stealthy hyperuniform systems, whether crystalline or disordered, since there are inevitable numerical inaccuracies. Moreover, in any experimental realization, there will be fabrication errors, measurement accuracy, and alignment errors between slabs that will inevitably lead to localization. Increasing the system size, dielectric contrast, or volume fraction amplifies the localization effects due to these inaccuracies.

As a result, the fundamental issue of whether disordered stealthy hyperuniform layered media in which the spectral density $\tilde{\chi}_v(k)$ is precisely zero for $0<k<K$ are truly transparent, *i.e.*, whether the localization length is finite or truly infinite, remains open. The question is equivalent to asking whether the imaginary part of the remainder term $\mathcal{R}_4(\omega)$, which embodies all contributions of fourth- and higher-order terms in the strong-contrast expansion within the predicted transparency interval [5,6], is exactly zero or small but positive in the thermodynamic limit. Resolving the issue is a theoretical challenge motivated by this study.

Even if a limiting localization length is ultimately established for the case of optical transmission through 1D layered media, our findings of no apparent evidence for localization for relatively large system sizes may be sufficient to exploit this property for practical applications of photonic and phononic material designs, such as low-pass filters and layered media for optical coatings, metasurfaces, integrated photonics, solar cells, or microelectromechanical systems. Another direction for future work is to combine the continuous apparent transparency regime of stealthy hyperuniform layered media with enhanced transmission via quasi-extended states as in Pendry's necklaces [53] or the random dimers introduced by Dunlap *et al.* [4].

Optical Materials EXPRESS

After this project was completed, a follow-up study [54] (that includes some of us) was initiated that investigated a rather different, *non-optical case* of coherent single-particle wave propagation in a lattice with Gaussian-distributed random on-site energies, where the Gaussian random field has a stealthy power spectrum in the sense that it vanishes over a continuous band of wave numbers. Because of the inherent Gaussianity, multiple-scattering contributions in the random field case can be calculated analytically such that it can be rigorously shown that there is "effective delocalization," cancellation of multiple scattering to arbitrary finite order. In contrast, the slab model has an exotic form of *positional* disorder, including the unusual non-Gaussian many-body "bounded-hole" property [12,13]. The Gaussian random field case may or may not have any bearing on the slab system, although its quite intriguing that both appear to produce similar effective delocalization effects based on the numerical calculations presented here. Taken together, the studies the two different systems open a new direction in Anderson localization studies aimed at determining which multiple-scattering properties are universal and which are model-specific in stealthy hyperuniform systems.

Methods

Samples of layered media To compare models with the same number of points per sample (10,000), we condition our simulation of RSA on the number of disks per sample (*i.e.*, we repeat the simulation until the prescribed number of points is obtained). We simulate the RSA points at a packing fraction of 37%. Then, we decorate these points with high-dielectric slabs with a volume fraction of $\phi = 1\%$.

We simulate the disordered stealthy hyperuniform samples using the collective coordinate optimization technique with a soft-core repulsion as in [38,39]. To preserve a high-degree of local disorder in our stealthy hyperuniform samples, we choose a maximum packing fraction of about 1.5%. We start from high-temperature initial conditions, more specifically, the ideal gas in the canonical ensemble. For the optimization of the collective coordinates, we employ a limited-memory Broyden–Fletcher– Goldfarb–Shanno (L-BFGS) optimization algorithm. To obtain high-quality 1D stealthy hyperuniform packings in a reasonable simulation time, we employ a three-step procedure. First, we simulate high-quality samples without soft-core repulsion with an energy tolerance of 10^{-17}; then, we repeat the simulation with soft-core repulsion with a radius of 0.015 and an energy tolerance of 10^{-8}; finally, we simulate high-quality samples without soft-core repulsion and an energy tolerance of again 10^{-17}. Although the last step is without soft-core repulsion, the remaining small collective displacements still preserve a volume fraction with $\phi = 1\%$ and do not create slab overlaps. For the equiluminous samples, we used an energy tolerance of 10^{-12} for the steps with hard-core repulsion.

All of our samples are simulated with periodic boundary conditions. For each model, we simulate at least 100 samples, except for the lattice where a single sample is representative. For the average transmission coefficients in Fig. 2 (bottom panel), we use 10,000 samples per model. For the phase diagram in Fig. 3, we simulate 30 samples for each χ value (for each of the 60 different χ values).

Transmission coefficients We use the transfer matrix methods as in [8]. For potential pitfalls, in a transmission coefficient analysis of localization with large system sizes, see Fig. S1 in the Supplement 1 text.

Localization analysis For a numerically stable Lyapunov analysis of localization, we use a QR-decomposition of the product of transfer matrices as in [44] or later in [46] with the help of the Householder transformation [55]. The algorithm decomposes each matrix in the product into an orthogonal and an upper-triangular matrix, Q and R, respectively. Based on the lattice case where we know $T = 1$ (or, equivalently, the localization length $\xi = 1/\lambda \to \infty$ as $L \to \infty$) and what we find numerically for the lattice for finite L, we infer that $1/\lambda_{\min}$ accurately gauges the localization length when L is large but finite. We then use $1/\lambda_{\min}$ to gauge the localization length

Optical Materials EXPRESS

for the disordered stealthy hyperuniform layered media, which have such similar behavior to the lattice for $\omega<\omega_c$, as illustrated in Figs. 5 and 6.

Due to the ripple effect that occurs in finite systems, the maximal numerical value of $\xi = 1/\lambda_{\min}$ is best determined by varying the range of L over a narrow range near its maximum value, which in this case is $L = 10,000$. In almost all cases, we have fixed this range to be $[9900, 10000]$, except for the case $\omega<0.1$, where the long wavelengths in the oscillations require extending the range to $[9500, 10000]$.

We minimize the Lyapunov exponent using a two-step procedure. First, we identify suitable candidates for sharp peaks (by sufficiently strong local minima in $\lambda(L)$); then, we iterate a golden-search minimization routine for each of these candidates (but stop the iteration if we find a functional value smaller than 10^{-15}). Note that just taking the smallest value of a preliminary search leads to systematic errors because of the strong oscillations in $\lambda(L)$ which may not always correspond to a sharp peak.

Note that the sharp peaks require a fine step size in L (for which we used 0.0001, where the unit of length is defined via $\rho = 1$). The oscillations in $\lambda(L)$ vary with shifts of the samples, which are subject to periodic boundary conditions. The shifts correspond to independent representations that result in different oscillations in $\lambda(L)$ because the product of transfer matrices does not use periodic boundary conditions. Therefore, we average over about 20 shifts for Fig. 3. The shifts should run over multiples of pairs of high-dielectric slabs for the disordered models. A sufficient number of shifts is required for good statistics (to not distort the Lyapunov exponent by a single outlier). Finally, we compute the average of λ_{min} over different samples.

We then use the median for each single sample to represent the dominant behavior of $\lambda_{\min}$ since the distribution of the numerically obtained values of $\lambda_{\min}$ is bimodal even for the perfect (periodic) lattice. For example, the median for the lattice accurately captures the perfect transmission. More precisely, the values of the Lyapunov exponent are either $O(10^{-15})$ (*i.e.*, zero within floating point precision) or $O(10^{-6})$ (depending on the system size and physical parameters). The median represents the dominant behavior and is less sensitive than the mean value to the precise protocol of our choice of shifts.

Funding. United States Army Research Office (W911NF-22-2-0103); Helmholtz Association of German Research Centres (VH-NG-19-34); Deutsche Forschungsgemeinschaft (KL 3391/2-2, WI 5527/1-1, LO 418/25-1).

Acknowledgment. We thank Jaeuk Kim for valuable discussions and his code for simulating disordered stealthy hyperuniform layered media. We also thank Luca Lotz for helpful discussions and suggestions. P. J. S. and S. T. acknowledge funding and support of the U.S. Army Research Office and was accomplished under Cooperative Agreement No. W911NF-22-2-0103. This work was also supported by the Initiative and Networking Fund of the Helmholtz Association under the call Helmholtz Young Investigator Groups (VH-NG-19-34, DataMat), as well as by the Deutsche Forschungsgemeinschaft (DFG, German Research Foundation) through SPP 2265 under Grant Nos. KL 3391/2-2, WI 5527/1-1, and LO 418/25-1. The simulations presented in this article were substantially performed on computational resources managed and supported by the Princeton Institute for Computational Science and Engineering (PICSciE). The authors also gratefully acknowledge the scientific support and HPC resources provided by the German Aerospace Center (DLR). The HPC system CARO is partially funded by "Ministry of Science and Culture of Lower Saxony" and "Federal Ministry for Economic Affairs and Climate Action."

Disclosures. The authors declare no conflicts of interest.

Data availability. The final data of this study will be made available in a Zenodo repository.

Supplemental document. See Supplement 1 for supporting content.

References

1. P. W. Anderson, "Absence of Diffusion in Certain Random Lattices," Phys. Rev. **109**(5), 1492–1505 (1958).
2. E. Abrahams, P. W. Anderson, D. C. Licciardello, *et al.*, "Scaling Theory of Localization: Absence of Quantum Diffusion in Two Dimensions," Phys. Rev. Lett. **42**(10), 673–676 (1979).
3. P. Sheng, *Introduction to Wave Scattering, Localization and Mesoscopic Phenomena*Springer Series in Materials Science (Springer-Verlag, Berlin Heidelberg, 2006), 2nd ed.
4. D. H. Dunlap, H.-L. Wu, and P. W. Phillips, "Absence of localization in a random-dimer model," Phys. Rev. Lett. **65**(1), 88–91 (1990).

Optical Materials EXPRESS

5. J. Kim and S. Torquato, "Effective electromagnetic wave properties of disordered stealthy hyperuniform layered media beyond the quasistatic regime," Optica **10**(8), 965–972 (2023).
6. J. Kim and S. Torquato, "Extraordinary optical and transport properties of disordered stealthy hyperuniform two-phase media," J. Phys.: Condens. Matter **36**(22), 225701 (2024).
7. P. Yeh, *Optical Waves in Layered Media* (Wiley, 1988).
8. H. A. Macleod, *Thin-Film Optical Filters* (CRC Press, Boca Raton, 2010), 4th ed.
9. S. Torquato and F. H. Stillinger, "Local density fluctuations, hyperuniformity, and order metrics," Phys. Rev. E **68**(4), 041113 (2003).
10. S. Torquato, "Hyperuniform states of matter," Phys. Rep. **745**, 1–95 (2018).
11. R. D. Batten, F. H. Stillinger, and S. Torquato, "Classical disordered ground states: Super-ideal gases and stealth and equi-luminous materials," J. Appl. Phys. **104**(3), 033504 (2008).
12. G. Zhang, F. H. Stillinger, and S. Torquato, "Can exotic disordered stealthy particle configurations tolerate arbitrarily large holes?" Soft Matter **13**(36), 6197–6207 (2017).
13. S. Ghosh and J. L. Lebowitz, "Generalized Stealthy Hyperuniform Processes: Maximal Rigidity and the Bounded Holes Conjecture," Commun. Math. Phys. **363**(1), 97–110 (2018).
14. M. Florescu, S. Torquato, and P. J. Steinhardt, "Designer disordered materials with large complete photonic band gaps," Proc. Natl. Acad. Sci. U.S.A. **106**(49), 20658–20663 (2009).
15. O. Leseur, R. Pierrat, and R. Carminati, "High-density hyperuniform materials can be transparent," Optica **3**(7), 763–767 (2016).
16. L. S. Froufe-Pérez, M. Engel, J. José Sáenz, *et al.*, "Transport Phase Diagram and Anderson Localization in Hyperuniform Disordered Photonic Materials," Proc. Natl. Acad. Sci. U.S.A. **114**(36), 9570–9574 (2017).
17. H. Zhang, H. Chu, H. Giddens, *et al.*, "Experimental demonstration of luneburg lens based on hyperuniform disordered media," Appl. Phys. Lett. **114**(5), 053507 (2019).
18. S. Gorsky, W. A. Britton, Y. Chen, *et al.*, "Engineered hyperuniformity for directional light extraction," APL Photonics **4**(11), 110801 (2019).
19. J. Haberko, L. S. Froufe-Pérez, and F. Scheffold, "Transition from light diffusion to localization in three-dimensional amorphous dielectric networks near the band edge," Nat. Commun. **11**(1), 4867 (2020).
20. N. Tavakoli, R. Spalding, A. Lambertz, *et al.*, "Over 65% sunlight absorption in a 1 μm si slab with hyperuniform texture," ACS Photonics **9**(4), 1206–1217 (2022).
21. M. A. Klatt, P. J. Steinhardt, and S. Torquato, "Wave propagation and band tails of two-dimensional disordered systems in the thermodynamic limit," Proc. Natl. Acad. Sci. **119**(52), e2213633119 (2022).
22. L. S. Froufe-Pérez, G. J. Aubry, F. Scheffold, *et al.*, "Bandgap fluctuations and robustness in two-dimensional hyperuniform dielectric materials," Opt. Express **31**(11), 18509–18515 (2023).
23. K. Vynck, R. Pierrat, R. Carminati, *et al.*, "Light in correlated disordered media," Rev. Mod. Phys. **95**(4), 045003 (2023).
24. A. Meek and M. Florescu, "Light propagation in one-dimensional stealthy hyperuniform disordered photonic structures," in *Nanophotonics X*, vol. 12991 (SPIE, 2024), pp. 314–320.
25. A. Meek and M. Florescu, "Electromagnetic Wave Localization in One-Dimensional Hyperuniform Disordered Structures," Adv. Opt. Mater. **14**(16), e03843 (2026).
26. G. Gkantzounis, T. Amoah, and M. Florescu, "Hyperuniform disordered phononic structures," Phys. Rev. B **95**(9), 094120 (2017).
27. V. Romero-García, N. Lamothe, G. Theocharis, *et al.*, "Stealth acoustic materials," Phys. Rev. Appl. **11**(5), 054076 (2019).
28. J. Kim and S. Torquato, "Multifunctional composites for elastic and electromagnetic wave propagation," Proc. Natl. Acad. Sci. U.S.A. **117**(16), 8764–8774 (2020).
29. H. Zhuang, D. Chen, L. Liu, *et al.*, "Vibrational properties of disordered stealthy hyperuniform 1d atomic chains," J. Phys.: Condens. Matter **36**(28), 285703 (2024).
30. M. Diego, J. Hardouin, G. Mazevet-Schargrod, *et al.*, "Hypersonic acoustic wave control via stealthy hyperuniform phononic nanostructures," Sci. Adv. **11**(32), eadw7205 (2025).
31. G. Zhang, F. H. Stillinger, and S. Torquato, "Transport, geometrical and topological properties of stealthy disordered hyperuniform two-phase systems," J. Chem. Phys. **145**(24), 244109 (2016).
32. S. Torquato and D. Chen, "Multifunctional hyperuniform cellular networks: optimality, anisotropy and disorder," Multifunct. Mater. **1**(1), 015001 (2018).
33. F. H. Alejandre, L. S. Froufe-Pérez, and F. Scheffold, "Transverse spreading Anderson Localization in two and three dimensional disordered correlated dielectric materials with bandgap regimes," EPJ Web Conf. **335**, 05020 (2025).
34. S. Torquato and J. Kim, "Nonlocal Effective Electromagnetic Wave Characteristics of Composite Media: Beyond the Quasistatic Regime," Phys. Rev. X **11**(2), 021002 (2021).
35. J. Park, S. Park, K. Kim, *et al.*, "Deep-subwavelength engineering of stealthy hyperuniformity," Nanophotonics **14**(8), 1113–1122 (2025).
36. S. N. Chiu, D. Stoyan, W. S. Kendall, *et al.*, *Stochastic Geometry and Its Applications* (Wiley, 2013), 3rd ed.
37. S. Torquato, *Random Heterogeneous Materials, vol. 16 of Interdisciplinary Applied Mathematics* (Springer, 2002), 2nd ed.

Optical Materials EXPRESS

38. J. Kim and S. Torquato, "Theoretical prediction of the effective dynamic dielectric constant of disordered hyperuniform anisotropic composites beyond the long-wavelength regime [Invited]," Opt. Mater. Express **14**(1), 194–215 (2024).
39. J. Kim and S. Torquato, "Ultradense Sphere Packings Derived From Disordered Stealthy Hyperuniform Ground States," J. Chem. Phys. **163**(2), 024902 (2025).
40. S. Torquato, G. Zhang, and F. H. Stillinger, "Ensemble Theory for Stealthy Hyperuniform Disordered Ground States," Phys. Rev. X **5**(2), 021020 (2015).
41. S. Torquato, "Disordered hyperuniform heterogeneous materials," J. Phys.: Condens. Matter **28**(41), 414012 (2016).
42. L. Dal Negro, *Waves in Complex Media: Fundamentals and Device Applications* (Cambridge university Press, New York, 2021).
43. S. M. Popoff, G. Lerosey, R. Carminati, *et al.*, "Measuring the Transmission Matrix in Optics: An Approach to the Study and Control of Light Propagation in Disordered Media," Phys. Rev. Lett. **104**(10), 100601 (2010).
44. K. Geist, U. Parlitz, and W. Lauterborn, "Comparison of Different Methods for Computing Lyapunov Exponents," Prog. Theor. Phys. **83**(5), 875–893 (1990).
45. M. V. Berry and S. Klein, "Transparent mirrors: Rays, waves and localization," Eur. J. Phys. **18**(3), 222–228 (1997).
46. J. A. Scales and E. S. Van Vleck, "Lyapunov Exponents and Localization in Randomly Layered Media," J. Comput. Phys. **133**(1), 27–42 (1997).
47. A. A. Chabanov, M. Stoytchev, and A. Z. Genack, "Statistical signatures of photon localization," Nature **404**(6780), 850–853 (2000).
48. J. D. Joannopoulos, S. G. Johnson, J. N. Winn, *et al.*, *Photonic Crystals: Molding the Flow of Light* (Princeton University Press, Princeton, 2008), 2nd ed.
49. S. Yu, C.-W. Qiu, Y. Chong, *et al.*, "Engineered disorder in photonics," Nat. Rev. Mater. **6**(3), 226–243 (2020).
50. H. Furstenberg, "Noncommuting Random Products," Trans. Amer. Math. Soc. **108**(3), 377–428 (1963).
51. I. Ya. Goldsheid, S. A. Molchanov, and L. A. Pastur, "A pure point spectrum of the stochastic one-dimensional schrödinger operator," Funct Anal Its Appl **11**(1), 1–8 (1977).
52. M. Aizenman and S. Molchanov, "Localization at large disorder and at extreme energies: An elementary derivation," Commun. Math. Phys. **157**(2), 245–278 (1993).
53. J. B. Pendry, "Quasi-extended electron states in strongly disordered systems," J. Phys. C: Solid State Phys. **20**(5), 733–742 (1987).
54. C. Vanoni, J. Karcher, M. C. Rechtsman, *et al.*, "Effective delocalization in the one-dimensional anderson model with stealthy disorder," Phys. Rev. Lett. **136**(15), 150404 (2026).
55. J.-P. Eckmann and D. Ruelle, "Ergodic theory of chaos and strange attractors," Rev. Mod. Phys. **57**(3), 617–656 (1985).